

## Superparamagnetic behavior of structural domains in epitaxial ultrathin magnetite films

F. C. Voogt,\* T. T. M. Palstra, L. Niesen, O. C. Rogojuanu, M. A. James, and T. Hibma  
*Materials Science Centre, University of Groningen, Nijenborgh 4, 9747 AG, Groningen, The Netherlands*  
 (Received 31 October 1997)

We provide evidence that thin films of magnetite  $\text{Fe}_3\text{O}_4$  epitaxially grown on single-crystalline  $\text{MgO}(100)$ , form domains with unique magnetic properties. Strong  $180^\circ$  Fe-O-Fe superexchange paths at antiphase domain boundaries result in a frustration of the interdomain interactions. Probe-layer Mössbauer spectroscopy shows superparamagnetic behavior in the entire film, in spite of the nearly perfect layer-by-layer growth. Superconducting quantum interference device magnetometry is used to determine the temperature and thickness dependence of the superparamagnetic blocking temperatures. [S0163-1829(98)00914-X]

Thin-film systems of magnetic transition metal oxides are under intense investigation at present, for their unique magnetic properties.<sup>1-3</sup> The combination of full spin polarization at the Fermi level and magnetic ordering temperatures above room temperature allow for the development of device concepts. Much recent work focuses on spin-polarized current injection.<sup>4,5</sup> This way, one intends to control the resistance of magnetic materials or the critical current of superconducting materials. However, the charge transport in oxides is determined by short-range interactions, typically between nearest or next-nearest neighbors. Therefore, the success of these concepts depends on the nature of the interfaces and surfaces of the materials. The structure in these regions can be different from the bulk by intrinsic effects, such as stress/strain, reconstructions, or by extrinsic effects, such as nonstoichiometry, interdiffusion, etc. Small variations can alter the magnetic behavior significantly. This makes a proper understanding of the surface/interface magnetic state indispensable. This state is not only critical for spin-polarized transport, but also for exchange biasing<sup>6,7</sup> or for the magnetic properties of ultrasmall particles.<sup>8</sup>

Only a few materials combine full spin polarization with high Curie temperatures ( $>300$  K): the manganese perovskites, the spinel  $\text{Fe}_3\text{O}_4$ ,  $\text{CrO}_2$ , and several Heusler compounds such as  $\text{PtMnSb}$ . In this paper, we focus on  $\text{Fe}_3\text{O}_4$ , a highly correlated material with a  $T_C$  of 858 K. There have been several reports of anomalous magnetic behavior. Studies on thin-film saturation magnetizations at room temperature showed a decrease, which was modeled with nonmagnetic or disordered, "dead" interface layers of 0.7 nm.<sup>9</sup> Such layers would render this material impractical for spin-polarized transport or exchange biasing. However, this interpretation is in disagreement with earlier depth-selective Mössbauer spectra of 50.0 and 100 nm-thick bulklike films.<sup>10</sup> The latter measurements indicated that the interface, surface, and bulk layers have the same magnetic properties, including the characteristic charge-ordering Verwey transition.

In this paper, it is shown that for ultrathin layers also ( $\leq 5$  nm), the properties of the surface and interface layers are not different from the interior, i.e., the dead layer model is invalidated. Instead, we will demonstrate that  $\text{Fe}_3\text{O}_4$  films, in the ultrathin limit, behave superparamagnetically. The origin of this superparamagnetism lies in the nucleation process of the  $\text{Fe}_3\text{O}_4$  films on  $\text{MgO}(100)$ . Although these epitaxial

films are single crystalline, because of the completely lattice matched growth, they will inherently contain antiphase boundaries.<sup>11</sup> The lower symmetry and the larger unit cell of the inverse spinel crystal structure, compared to the rock-salt structure, result in that an  $\text{Fe}_3\text{O}_4$  island can nucleate on  $\text{MgO}(100)$  in eight unique ways. As shown in Fig. 1, antiphase boundaries are the result of the coalescence of islands, which are either rotated over  $90^\circ$  with respect to each other, or shifted, or both. Such antiphase boundaries have recently been made visible by scanning tunnel microscope (STM) imaging of molecular-beam epitaxy (MBE) grown  $\text{Fe}_3\text{O}_4$  layers on  $\text{MgO}(100)$ .<sup>12</sup> Consequently, the layer will

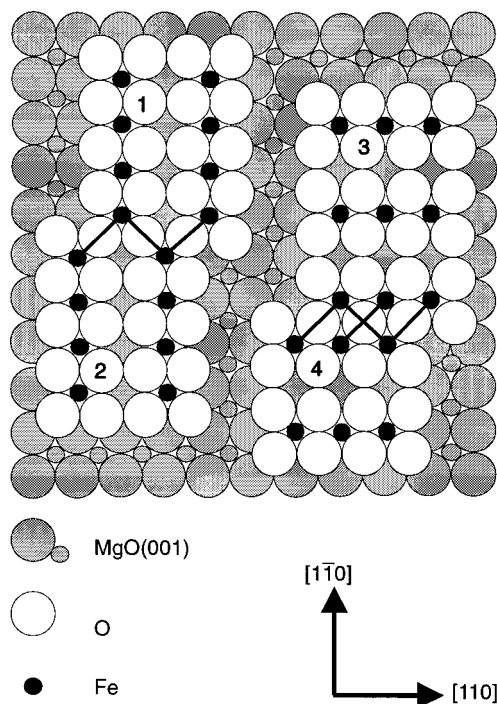


FIG. 1. Schematic representation of the formation of an  $\text{Fe}_3\text{O}_4$  film on  $\text{MgO}(100)$ . For clarity, only one monolayer, containing only octahedral Fe cations, is shown. The coalescence of islands 1 with 2, and 3 with 4, which are shifted with respect to each other, leads to new antiferromagnetic  $180^\circ$  Fe-O-Fe superexchange paths at the antiphase boundaries, as indicated with solid lines. The same paths arise after coalescence of islands, which are rotated over  $90^\circ$  with respect to each other (islands 1,2 with 3,4).

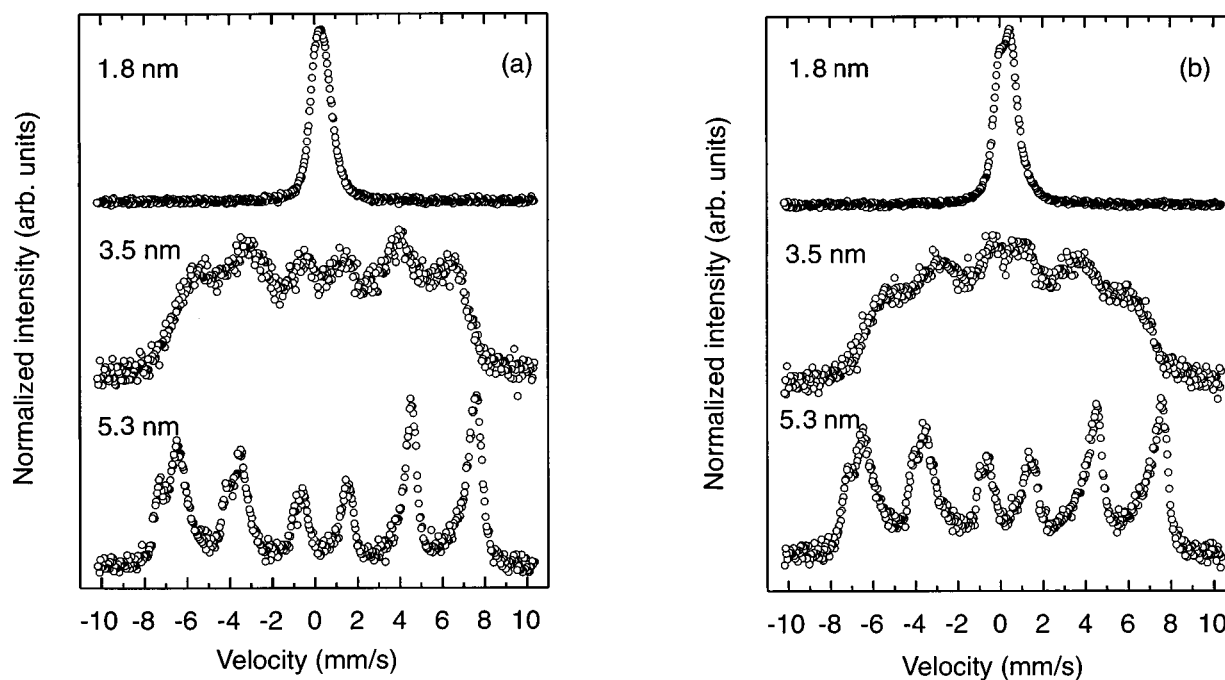


FIG. 2. Room-temperature conversion electron Mössbauer spectra (CEMS) of (100)  $\text{Fe}_3\text{O}_4/\text{MgO}$  multilayers, as a function of  $\text{Fe}_3\text{O}_4$  layer thickness (indicated above each spectrum), and  $^{57}\text{Fe}$  probe position: (a) in the center of the  $\text{Fe}_3\text{O}_4$  layer, and (b) at the  $\text{Fe}_3\text{O}_4/\text{MgO}$  interface.

have a continuous  $\text{O}^{2-}$  sublattice, but a fragmented cation sublattice.  $\text{Fe}_3\text{O}_4$  thin films should, therefore, be regarded as a patchwork of domains.

We will provide evidence that this domain structure leads to a unique form of superparamagnetism. The bulklike exchange interactions are interrupted at the antiphase boundaries, which causes the crystallographic domains to act like magnetic domains. These domains can change their magnetization direction with thermal activation energies.

To investigate the magnetic properties of ultrathin  $\text{Fe}_3\text{O}_4$  films, we have adopted the technique from Ref. 10. Multilayer samples were made consisting of 5  $\text{Fe}_3\text{O}_4$  layers, separated and capped by 2.0 nm-thick MgO layers. Three different  $\text{Fe}_3\text{O}_4$  layer thicknesses were studied, i.e., 1.8, 3.5, and 5.3 nm. Each  $\text{Fe}_3\text{O}_4$  layer consisted of a probe layer of 0.42 nm (2 monolayers) grown with the Mössbauer active isotope  $^{57}\text{Fe}$ , positioned in a matrix grown with natural Fe. By locating this probe layer either at the  $\text{Fe}_3\text{O}_4/\text{MgO}$  interface or in the center of the  $\text{Fe}_3\text{O}_4$  layer, position-specific information concerning the magnetic properties could be obtained. We point out that the function of the multilayer structure is merely to enhance the  $\text{Fe}_3\text{O}_4$  signal. The MgO spacer thickness is large enough to exclude exchange coupling between successive  $\text{Fe}_3\text{O}_4$  layers via ferrimagnetic bridges.<sup>13</sup>

The multilayers have been grown epitaxially on *ex situ* cleaved single crystalline MgO(100) substrates, by means of  $\text{NO}_2$ -assisted MBE. Details concerning this growth technique can be found in Ref. 14. Both oxides grow perfectly lattice matched on top of each other, with (100) orientations and a parallel alignment of the  $\langle 100 \rangle$  cubic crystal axes. Moreover, we always observe strong and persistent reflection high-energy electron diffraction intensity oscillations during deposition, which is a fingerprint of layer-by-layer growth. This conclusion is not only reached from our work, but also by

research from several other groups (see Ref. 15). Therefore, we stress that the films are not poly, but single crystalline, with atomically flat interfaces.

The structural quality of the multilayers was checked with x-ray specular reflectivity measurements. Apart from the bulk Bragg peaks, the spectra clearly show superlattice peaks, due to the  $\text{Fe}_3\text{O}_4/\text{MgO}$  bilayer repeat unit, and smaller secondary maxima, due to the total multilayer thickness. The  $\text{Fe}_3\text{O}_4$  layer thicknesses mentioned in this paper have been obtained from fits to these spectra. For the interface roughnesses, we find values of  $\sim 0.3$  nm, which correspond to only 1–2 monolayers.

Figure 2 shows room-temperature conversion electron Mössbauer spectra (CEMS) as a function of the  $\text{Fe}_3\text{O}_4$  layer thickness and  $^{57}\text{Fe}$  probe position. Two features of the spectra directly catch the eye. First, as the layer thickness decreases, there is a transition from a static configuration to a phase where the magnetic spins are fluctuating very rapidly. For the two 5.3 nm samples, the spectra show two hyperfine-split sextets, originating from the long-range ferrimagnetic order in  $\text{Fe}_3\text{O}_4$ .<sup>10</sup> The hyperfine fields are smaller than those of the bulk, already indicating enhanced fluctuations for this thickness. In the case of the thinnest layers (1.8 nm), the spectra are completely motionally narrowed, showing only one single line. Here, the Fe magnetic spins are fluctuating at least two orders of magnitude faster than the Larmor precession frequency of the nuclear spins ( $\sim 10^8$  Hz). Typical relaxation behavior is found for the two 3.5 nm samples. In this intermediate case, the spins are fluctuating on the same time scale as the Larmor period.

Second, probe layers at the interface and in the interior have similar magnetic properties. As can be seen in Fig. 2, the shape of the spectra only depends on the layer thickness, and not on the probe position. This observation, together

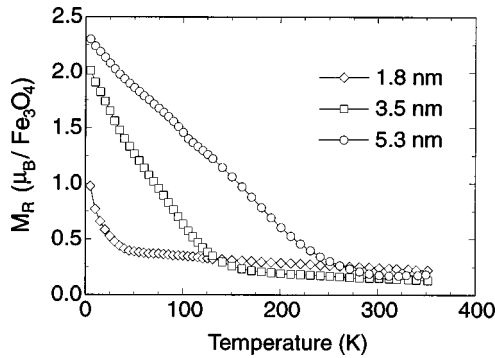


FIG. 3. Remanent magnetization  $M_R$ , in units of  $\mu_B$  per formula unit  $\text{Fe}_3\text{O}_4$ , of  $\text{Fe}_3\text{O}_4/\text{MgO}$  multilayers, after saturation in an external field of 1 T at 5 K, as a function of temperature and  $\text{Fe}_3\text{O}_4$  layer thickness.

with similar observations reported for 50.0 and 100.0 nm-thick bulklike layers,<sup>10</sup> rules out the idea of magnetically inactive, dead layers, sandwiching a ferrimagnetic interior. Instead, the  $\text{Fe}_3\text{O}_4$  layer behaves as a single magnetic entity for all thicknesses. We point out that the broad parabolic background in the case of probe layers situated at the interface corresponds to the outermost atomic plane in the  $\text{Fe}_3\text{O}_4$  layer. The  $\text{Fe}^{2+}$  and  $\text{Fe}^{3+}$  ions in this monolayer have a reduced number of nearest neighbors, resulting in a weakened ferrimagnetic ordering. The parabolic shape of this background probably arises from a broad distribution of reduced hyperfine fields.<sup>10</sup>

In bulk  $\text{Fe}_3\text{O}_4$ , the dominant superexchange interaction between nearest-neighbor  $A$ - $B$  ions is quite strong, i.e.,  $J_{AB} = -23.4$  K,<sup>16</sup> leading to a high ferrimagnetic ordering temperature  $T_C$  of 858 K.<sup>17</sup> This excludes a description in terms of individually fluctuating spins, i.e., paramagnetism. Therefore, the observed fluctuations must be collective spin fluctuations of entire domains, i.e., the thin films are *superparamagnetic*.

Complementary evidence was obtained with superconducting quantum interference device (SQUID) magnetometry measurements (MPMS-7, Quantum Design). In the inverse spinel structure of  $\text{Fe}_3\text{O}_4$ , the antiparallel coupling of the  $A$ - and  $B$ -site sublattices yields formally one uncompensated  $\text{Fe}^{2+}$  spin per formula unit  $\text{Fe}_3\text{O}_4$ , with a magnetic moment of  $4.1\mu_B$ .<sup>17</sup> At 25 K, all multilayers can be magnetized to saturation in external fields of 0.5 T, yielding magnetic moments of 4.9, 5.2, and  $4.5\mu_B/\text{Fe}_3\text{O}_4$  for thicknesses of 1.8, 3.5, and 5.3 nm, respectively. This indicates that the local coordination in the thin films is the same as in the bulk, preserving the magnetic moments of all Fe ions. Again, this contradicts the dead layer model. It is not clear why the moments are larger than the bulk value of  $4.1\mu_B$ . Most likely, it is related to the large uncertainties that arise when the relatively large diamagnetic and paramagnetic contributions of the substrate are subtracted from the small signal of the multilayer.

The superparamagnetic nature becomes evident from the behavior of the remanent magnetization,  $M_R$ . In Fig. 3,  $M_R$  is shown as a function of temperature for the three film thicknesses. These data were obtained by monitoring  $M_R$  while heating the samples, after saturating the magnetization in a field of 1 T at 5 K. Whereas bulk  $\text{Fe}_3\text{O}_4$  has a high  $T_C$  of 858

K,  $M_R$  rapidly vanishes for the thin films. The monotonous decrease of  $M_R$  with temperature indicates superparamagnetic relaxation. The point where the  $M_R$  curves level off can be identified as the maximum blocking temperature,  $T_B$ . This gives values of 40, 140, and 250 K for the 1.8, 3.5, and 5.3 nm thick films, respectively.

The decay of  $M_R$  is governed by the relaxation time  $\tau$ , the time to reverse the domain magnetization over a barrier with a height  $W$ . In a simple activated model, we can write<sup>18</sup>  $\tau = \tau_0 \exp(W/kT)$ , where  $\tau_0^{-1}$  is the attempt frequency ( $\sim 10^{11}$  Hz). It follows that the observed  $T_B$  depends on the timescale of the measurement,  $\tau_m$ . If  $\tau \ll \tau_m$ , the system behaves superparamagnetically, and if it is the other way around, we observe the blocked state. By definition,  $\tau = \tau_m$  at  $T_B$ . Given the difference in  $\tau_m$  for CEMS and SQUID magnetometry, i.e.,  $\sim 10^{-8}$  vs  $\sim 10^2$  s,  $T_B$  observed with CEMS should be 175, 600, and 1080 K, for the three films. This is in reasonable agreement with our data, i.e., the 1.8 nm films behave fully paramagnetic, the 3.5 nm films are approaching  $T_B$ , and the 5.3 nm films are in the blocked state. Note, that with SQUID we have determined the maximum values of  $T_B$ . These have to be considered as the upper limit of a broad distribution.

We attribute the superparamagnetic behavior to thermal fluctuations of the magnetic moments of structural domains. To demonstrate that these domains can indeed change the orientation of their magnetization with thermal activation energies, we will evaluate the various barrier heights for fluctuation. These depend on intrinsic properties of the domains, and also on the interaction between them.<sup>18</sup> We will consider domains in the thinnest film, assuming a columnar, rectangular shape with lateral dimensions of roughly  $\sim 10$  nm.<sup>12</sup> The following three barriers are considered:

(i) *Magneto-crystalline anisotropy energy*. The barrier in the film plane is given by  $W_a = K_1 V/4$ , with  $K_1 = 13$  kJ/m<sup>3</sup> (Ref. 9) and  $V$  the volume of the domain. This leads to  $W_a \approx 4$  meV.

(ii) *Magnetic dipole-dipole interactions between domains*. Following the model of Dormann *et al.*<sup>18</sup> for interacting ferrimagnetic particles, we estimate this contribution to be  $W_d = \mu_0 M^2 V \sum_j n_j a_j - kT \sum_j n_j$ , where the summation is over all neighboring domains. Here,  $a_j = (3 \cos^2 \theta_i - 1)V/d_i^3$ , with  $\theta_i$  and  $d_i$  the polar angle and length of the position vector of domain  $i$  with respect to the origin domain, taking the domain magnetization  $M$  as the  $z$  axis ( $M = 497$  kA/m, Ref. 9). Considering arrangements of four up to eight nearest and next-nearest-neighbor domains, we find that  $W_d \approx 0.15$  eV at  $T_B = 40$  K.

From (i) and (ii), it follows that the volume of the domains is indeed small enough to induce superparamagnetism. The resultant barrier is comparable to the maximum barrier height of 0.10 eV, as derived from SQUID magnetometry. However, since the films are single crystalline, we must consider a third barrier:

(iii) *Superexchange interactions at antiphase boundaries*. This barrier arises because the domains are fully intergrown. In order to estimate its importance, we have analyzed the structure and properties of all possible antiphase boundaries. During the layer-by-layer growth of  $\text{Fe}_3\text{O}_4$  on  $\text{MgO}(100)$ , stacking faults will appear in the first monolayer, with  $\langle 110 \rangle$

directions. The STM images of Ref. 12 indicate that these are the preferred orientations of the step edges. In the spinel structure, the orientation of the subsequent monolayers is determined by the orientation of the first monolayer. Therefore, the stacking faults will extend in all subsequent monolayers, resulting in planar antiphase boundaries with  $\{110\}$  orientations. The domains will have a rectangular and columnar shape, and a volume that increases linear with the film thickness. We point out that, in a multilayer structure, layer-by-layer growth on MgO and the accompanying stacking fault formation will occur in every  $\text{Fe}_3\text{O}_4$  layer. Therefore, all layers will have similar domain structures. However, the intermediate MgO layers are single domain, like the substrate. Therefore, antiphase boundaries in one  $\text{Fe}_3\text{O}_4$  layer cannot extend into the other layers, i.e., they are not correlated.

Most important, we find that the network of exchange interactions in  $\text{Fe}_3\text{O}_4$  is altered at the antiphase boundaries. There are new, strong  $180^\circ$  Fe-O-Fe superexchange paths between octahedral cations, across the boundary plane. These  $180^\circ$  paths, not present in bulk  $\text{Fe}_3\text{O}_4$ , originate from an intertwining of  $\langle 110 \rangle$  octahedral cation chains from two domains, which do not match at the antiphase boundary (see Fig. 1). They are present in every monolayer, all over the boundary plane. Also normal  $J_{AB}$  couplings are present, but they are usually outnumbered by the new  $180^\circ$  couplings. Therefore, the resultant coupling between two domains turns out to be either frustrated or, in most cases, antiferromagnetic. Only when two islands with matching orientations meet, the resultant coupling between the two domains is ferromagnetic. However, this event, with a probability of only  $\frac{1}{8}$ , is equivalent to the formation of 1 larger domain out of two smaller ones, without an internal boundary.

The estimated exchange constant  $J$  of the  $180^\circ$  Fe-O-Fe interaction is  $-25$  K,<sup>19</sup> which is of the same magnitude as the bulk  $J_{AB}$  coupling of  $\text{Fe}_3\text{O}_4$ . Given the interaction energy

$U_{ij} = -2J_{ij}S_i S_j$ , with  $S = 2$  or  $\frac{5}{2}$ , and an average number of  $3 \times 10^{19} \text{ m}^{-2}$  superexchange interactions between neighboring domains, this leads to  $W_{\text{ex}} \approx 3 \times 10^1 \text{ eV}$  per 10 nm length of antiphase boundary.

Comparing this estimate with the experimental data, we conclude that the influence of the huge superexchange barriers must be largely suppressed in the thin films. This can be explained by domain frustration. The new  $180^\circ$  Fe-O-Fe interactions play a crucial role in this, because they lead to antiferromagnetic coupling between domains. If all couplings were ferromagnetic, a domain would be rigidly locked, and superparamagnetism would not be observed at all. Antiferromagnetic coupling, however, unavoidably leads to frustration, similar to the situation in a spin glass. The superexchange barriers effectively cancel each other out, enabling the domains to fluctuate much more freely. Thus, the single crystalline film becomes superparamagnetic.

To conclude, it was shown that the  $\text{Fe}_3\text{O}_4$  layer behaves as one magnetic entity for all thicknesses, without dead or non-magnetic interface layers. The anomalous magnetic behavior, generally observed for ultrathin  $\text{Fe}_3\text{O}_4$  (100) films, is caused by a superparamagnetic state of the film. This finding is essential for the interpretation of studies on exchange biasing, magnetic interlayer coupling, and magnetic interface anisotropy. Furthermore, it will open up again the large potential of this material for application in spin electronics devices. Since similar arguments apply, the superparamagnetic behavior is also expected to occur in epitaxial films with other orientations, such as (110) and (111). Furthermore, it is not restricted to  $\text{Fe}_3\text{O}_4$ , but can occur in all spinel ferrite films grown on rocksalt-type substrates such as MgO, NiO, or CoO, depending on the strength of the  $180^\circ$  superexchange interactions.

We thank G. A. Sawatzky and T. Fujii for valuable comments, and J. Baas for his help with the SQUID magnetometry measurements.

\*Author to whom correspondence should be addressed. Electronic address: VOOGT@PHYS.RUG.NL

<sup>1</sup>N. D. Mathur *et al.*, Nature (London) **387**, 266 (1997).

<sup>2</sup>A. Gupta *et al.*, Phys. Rev. B **54**, R15 629 (1996).

<sup>3</sup>Y. Suzuki *et al.*, Appl. Phys. Lett. **68**, 714 (1996).

<sup>4</sup>H. Y. Hwang *et al.*, Phys. Rev. Lett. **77**, 2041 (1996).

<sup>5</sup>J. Z. Sun *et al.*, Appl. Phys. Lett. **69**, 3266 (1996).

<sup>6</sup>P. J. van der Zaag *et al.*, J. Appl. Phys. **79**, 5103 (1996).

<sup>7</sup>Y. Suzuki *et al.*, Phys. Rev. B **53**, 14 016 (1996).

<sup>8</sup>R. H. Kodama *et al.*, Phys. Rev. Lett. **77**, 394 (1996).

<sup>9</sup>P. A. A. van der Heijden *et al.*, J. Magn. Magn. Mater. **159**, L293 (1996).

<sup>10</sup>T. Fujii *et al.*, J. Magn. Magn. Mater. **130**, 267 (1994).

<sup>11</sup>D. M. Lind *et al.*, J. Appl. Phys. **73**, 6886 (1993); J. A. Borchers *et al.*, Phys. Rev. B **51**, 8276 (1995); D. T. Margulies *et al.*, *ibid.* **53**, 9175 (1996).

<sup>12</sup>J. M. Gaines *et al.*, Surf. Sci. **373**, 85 (1997).

<sup>13</sup>P. A. A. van der Heijden *et al.*, Phys. Rev. B **55**, 11 569 (1997).

<sup>14</sup>F. C. Voogt *et al.*, Surf. Sci. **331-333**, 1508 (1995); Hyperfine Interact. **97/98**, 99 (1996); J. Cryst. Growth **174**, 440 (1997).

<sup>15</sup>D. M. Lind *et al.*, Phys. Rev. B **45**, 1838 (1992); R. M. Wolf *et al.*, Mater. Res. Soc. Symp. Proc. **341**, 23 (1994); Y. J. Kim, Y. Gao, and S. A. Chambers, Surf. Sci. **371**, 358 (1997).

<sup>16</sup>C. M. Srivastava, G. Srinivasan, and N. G. Nanadikar, Phys. Rev. B **19**, 499 (1979).

<sup>17</sup>J. Smit and H. P. J. Wijn, *Ferrites* (Philips Technical Library, Eindhoven, 1959).

<sup>18</sup>J. L. Dormann *et al.*, Phys. Rev. B **53**, 14 291 (1996).

<sup>19</sup>K. Motida and S. Miyahara, J. Phys. Soc. Jpn. **28**, 1188 (1970); C. Boekema, F. van der Woude, and G. A. Sawatzky, Int. J. Magn. **3**, 341 (1971).